Catalysis Letters
https://doi.org/10.1007/s10562-019-02923-3

Metal Cocatalyst Directing Photocatalytic Acetonylation of Toluene via Dehydrogenative Cross-Coupling with Acetone

Akanksha Tyagi[1] · Tomoya Matsumoto[2] · Akira Yamamoto[1,2] · Tatsuhisa Kato[2,3] · Hisao Yoshida[1,2]

Received: 18 May 2019 / Accepted: 29 July 2019

Abstract

A heterogeneous metal-loaded titanium oxide photocatalyst provided an efficient route to bring out direct dehydrogenative cross-coupling between toluene and acetone without consuming any additional oxidizing agent. The nature of the metal nanoparticle cocatalyst deposited on TiO_2 photocatalyst dictated the product selectivity for the cross-coupling. Pd nanoparticles on TiO_2 photocatalyst allowed a C–C bond formation between the aromatic ring of toluene and acetone to give 1-(*o*-tolyl) propan-2-one (**1a1**) with high regioselectivity, while Pt nanoparticles on TiO_2 photocatalyst promoted the cross-coupling between the methyl group of toluene and acetone to give 4-phenylbutan-2-one (**1b**) as the acetonylated product. These results demonstrated that the selection of the metal cocatalyst on TiO_2 photocatalyst could determine which C–H bonds in toluene, aromatic or aliphatic, can react with acetone. Two kinds of reaction mechanisms were proposed for the photocatalytic dehydrogenative cross-coupling reaction, depending on the property of the metal nanoparticles, i.e., only Pd nanoparticles can catalyze the reaction between aromatic ring and the acetonyl radical species.

Graphic Abstract

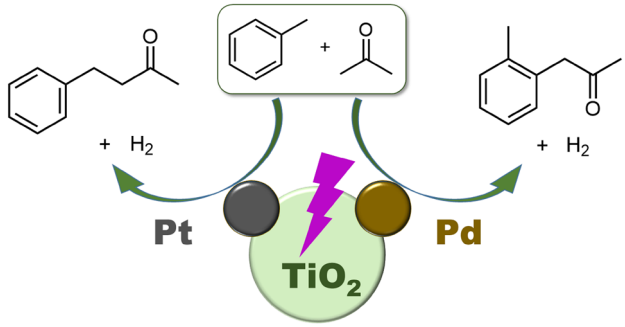

Keywords Titanium oxide · Photocatalysis · C–C cross-coupling · Reaction mechanism · Dehydrogenative cross-couplings

Electronic supplementary material The online version of this article (https://doi.org/10.1007/s10562-019-02923-3) contains supplementary material, which is available to authorized users.

✉ Hisao Yoshida
yoshida.hisao.2a@kyoto-u.ac.jp

[1] Elements Strategy Initiative for Catalysts and Batteries (ESICB), Kyoto University, Kyotodaigaku-Katsura, Nishikyo-ku, Kyoto 615-8520, Japan

[2] Graduate School of Human and Environmental Studies, Kyoto University, Yoshida Nihonmatsu-cho, Sakyo-ku, Kyoto 606-8501, Japan

[3] Institute for Liberal Arts and Sciences (ILAS), Kyoto University, Yoshida Nihonmatsu-cho, Sakyo-ku, Kyoto 606-8501, Japan

Published online: 12 August 2019

1 Introduction

TiO_2 photocatalysis has been well examined for the mitigation of various energy and environmental issues like hydrogen production for renewable energy by water splitting [1–3], CO_2 reduction [4–6], and air and water purification by the degradation of organic pollutants [7, 8]. The selective organic reactions like C–C couplings, on the contrary, are still infancy [9, 10]. The photoirradiation of TiO_2 generates electrons and holes in the conduction and valence bands that can oxidize and reduce different organic molecules or ions to form the corresponding radical species. So far, many reports have shown that a careful selection of the substrates [11–13], controlling the morphology of the photocatalyst [14–16], or the deposition of cocatalysts on the photocatalyst [17–19] can notably improve the selectivity in these TiO_2 catalyzed organic reactions [20]. Particularly, cocatalysts, which are usually responsible for the charge separation on TiO_2, can significantly affect the selectivity of the photocatalytic reactions [21–24].

In the present work, we report the selective photocatalytic activation of the C–H bonds in arenes by a heterogeneous metal-loaded TiO_2 photocatalyst (M/TiO_2) to carry out the acetonylation of toluene via a direct dehydrogenative cross-coupling (DCC) with acetone, where a C–H bond of toluene and that of acetone are cleaved to make a new C–C bond with the concomitant release of hydrogen gas without consuming any additional oxidizing agent. The products are arylacetones, a common precursor to medicinal compounds like amphetamine [25]. Thus, our study provides a simple and sustainable methodology over the commonly used methods [26–28] to prepare arylacetones. In this study, it was found that the nature of the metal nanoparticles loaded on TiO_2 photocatalyst significantly affected the product selectivity. The Pd-loaded TiO_2 sample (Pd/TiO_2) promoted the DCC between the aromatic ring of toluene and acetone to give ortho and para substituted products namely, 1-(*o*-tolyl)propan-2-one (**1a1**) and 1-(*p*-tolyl) propan-2-one (**1a2**) majorly. The Pt/TiO_2 sample, in contrast, promoted the cross-coupling between the methyl groups of both toluene and acetone to give 4-phenylbutan-2-one (**1b**) (Scheme 1). A systematic study revealed that the formation of the two types of products, i.e., aromatic substituted and methyl substituted, follows different mechanistic routes that require the different abilities of the deposited metal cocatalysts. Thus, by choosing the suitable metal cocatalyst, we achieved the selective activation of C–H bonds in toluene and consequently the DCC with acetone.

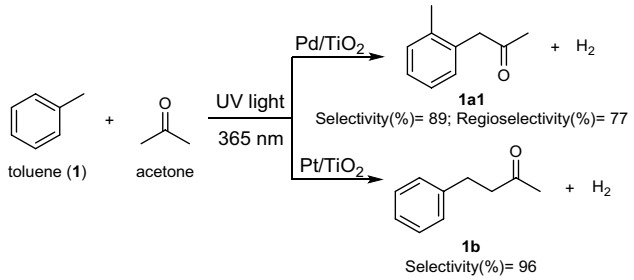

Scheme 1 Direct photocatalytic DCC between toluene and acetone with different M/TiO_2 samples. The reaction conditions were same as those mentioned in Table 1

2 Experimental Section

2.1 Catalyst Preparation

The metal-loaded titanium oxide photocatalysts (M(*x*)/TiO_2, M: Pd, Pt, Au, *x*: loading amount in wt%) were prepared by a photodeposition method. The TiO_2 sample was obtained from Catalysis Society of Japan (JRC-TIO-8, 338 m^2g^{-1}). 4 g of this sample was dispersed in 300 mL ion-exchanged water and stirred under the light irradiation from a xenon lamp (PE300BUV) for 30 min. Then, 100 mL methanol and desired volume of the metal precursor solution ($PdCl_2$ for Pd, $H_2PtCl_6{\cdot}6H_2O$ for Pt, and $HAuCl_4{\cdot}4H_2O$ for Au) were added and the resultant suspension was stirred in the dark for 15 min and under the light irradiation for 1 h. The suspension was filtered, washed with ion-exchanged water, and dried at 326 K for 12 h, which provided a M(*x*)/TiO_2 (M = Pd, Pt, or Au) photocatalyst. The Rh- and Ru-loaded TiO_2 samples [Rh(0.5)/TiO_2 and Ru(0.5)/TiO_2] were prepared by an impregnation method. 4 g of the JRC TIO-8 sample was dispersed in 100 mL ion-exchanged water and stirred at room temperature for 10 min. Then, the desired volume of the metal precursor solution ($RhCl_3{\cdot}6H_2O$ for Rh and $RuCl_3{\cdot}3H_2O$ for Ru) was added and the suspension was heated at 363 K to evaporate the water to dryness. After drying for 12 h at 326 K in an electric oven, the resultant powder was calcined at 723 K for 1 h to get the M(0.5)/TiO_2 (M = Rh or Ru) samples.

2.2 Photocatalytic Activity Test

All chemicals were of analytical grade and used without any further purification; toluene (Kishida Chemicals), aniline (Kishida Chemicals), *o*-toluidine (Wako Pure Chemicals), benzylamine (Nacalai Tesque), acetone (Nacalai Tesque), acetophenone (Wako Pure Chemicals),

1-(*o*-tolyl)propan-2-one (Aldrich), 1-(*p*-tolyl)propan-2-one (Alfa Aesar), toluene-d_8 (Aldrich), and acetone-d_6 (TCI Chemicals). The photocatalytic reaction tests were done in a Pyrex test tube (70 mL) as a closed reactor, under argon atmosphere. Typical conditions are mentioned here. At first, the photocatalyst (0.1 g) was irradiated under the light from the xenon lamp to clean up its surface. Then, the reactants (4.0 mL in total) were added and the test tube was sealed with a silicon septum and purged with a flow of argon gas for 10 min and stirred under the light irradiation for 3 h (the wavelength of the incident light was 365 ± 20 nm, the irradiation area was 4.95 cm^2, and the intensity was 180 mW cm^{-2}). After the photoirradiation, a part of the gas phase (0.5 mL) was taken in a gas-tight syringe and analyzed by GC-TCD (Shimadzu, GC-8A). The reaction mixture was filtered by using a syringe equipped with a PTFE filter, diluted with a solvent, including an internal standard (*n*-decane), and then analyzed by GC–MS (QP5050A).

3 Results and Discussion

3.1 Photocatalytic Reaction

Table 1 shows the results of the screening of the photocatalysts for the dehydrogenative acetonylation of toluene with acetone. The reaction gave three products, 1-(*o*-tolyl)propan-2-one (**1a1**), 1-(*p*-tolyl)propan-2-one (**1a2**), and 4-phenylbutan-2-one (**1b**). The reaction also gave some homo-coupling products from toluene like 1,2-diphenylethane, whose amount was minimized in the suitable reaction conditions. Also detected was 4-hydroxy-4-methylpentan-2-one as an aldol condensation product, which can be catalyzed by the acidic property of TiO_2 surface. Although hydrogen was detected in the gas phase, the amount of hydrogen and the DCC products was not balanced, which is probably due to side reactions [29–32].

The reaction done with the bare TiO_2 sample gave only **1b** and the aromatic DCC did not proceed (Table 1, entry 1). Among the different metal cocatalysts screened on the TiO_2 photocatalyst, the Pd and Pt cocatalysts gave the largest amount of the DCC products (Table 1, entries 2–6). The Au- and Ru-loaded TiO_2 samples showed low activity while the Rh-loaded sample was inactive for these reactions. The products were not obtained in the reaction carried out in the dark or without the TiO_2 photocatalyst under the light irradiation, supporting that the DCC products were photocatalytically obtained (Table 1, entries 7 and 8, respectively).

Interestingly, the selectivity to the DCC products varied with the metal cocatalyst deposited on the TiO_2 photocatalyst. The DCC products should be divided into two: **1a1** and **1a2** were the products of the cross-coupling between the aromatic ring of toluene and acetone, while **1b** was that with the methyl group of toluene. The selectivity *S* (%) to aromatic DCC products is shown in Table 1. Among the two aromatic DCC products (**1a1** and **1a2**), the regioselectivity to **1a1**, defined as *R* (%) and also listed, was high in all reactions ($R \geq 75\%$). Methyl group is an electron donating group which has an induction effect (+I) at *ortho* and *para* positions. This effect is stronger at *ortho* position than *para*, resulting in higher regioselectivity to **1a1** over **1a2**. While

Table 1 Direct photocatalytic DCC between toluene and acetone with different photocatalysts

Entry	Photocatalyst	Products (μmol)				*S* (%)[a]	*R* (%)[b]
		1a1	**1a2**	Sum of **1a1** + **1a2**	**1b**		
1	TiO_2	0.00	0.00	0.00	0.53	0	–
2	Pd(0.5)/TiO_2	1.23	0.36	1.59	0.19	89	77
3	Pt(0.5)/TiO_2	0.15	0.03	0.18	1.19	13	82
4	Au(0.5)/TiO_2	0.06	0.00	0.06	0.60	9	100
5	Ru(0.5)/TiO_2	0.00	0.00	0.00	0.29	0	–
6	Rh(0.5)/TiO_2	0.00	0.00	0.00	0.00	–	–
7[c]	Pd(0.5)/TiO_2	0.00	0.00	0.00	0.00	–	–
8[d]	None	0.00	0.00	0.00	0.00	–	–
9	Pd(5.0)/TiO_2	8.04	2.69	10.73	0.74	94	75

Reaction conditions: 0.1 mL (0.94 mmol) of toluene, 3.9 mL (52.6 mmol) of acetone, 0.1 g of M(*x*)/TiO_2 photocatalyst were used for a 3 h reaction. Wavelength of the irradiated light: $\lambda = 365 \pm 20$ nm, light intensity I = 180 mW cm^{-2} (measured at 365 ± 20 nm)

[a]Selectivity (%) to aromatic DCC products: $S\ (\%) = 100 \times$ [sum of the amounts of **1a1** and **1a2** (μmol)/total amount of acetonylated products (μmol)]

[b]Regioselectivity (%) to **1a1**: $R\ (\%) = 100 \times$ [amount of **1a1** (μmol)/sum of **1a1** and **1a2** (μmol)]

[c]The reaction was carried out in the dark

[d]The reaction was carried out without any photocatalyst under the light irradiation

the Pd cocatalyst promoted the DCC reaction between the aromatic ring and acetone with high selectivity ($S = 89\%$) and high regioselectivity ($R = 77\%$) to give **1a1** (Table 1, entry 2), other metals like Pt promoted the DCC reaction at the methyl group of toluene to give **1b** with high selectivity ($S = 13\%$) (Table 1, entry 3). These results indicate that the metal nanoparticles on the TiO_2 photocatalyst play an important role in the photocatalytic reaction that governs the product selectivity. The amount of Pd on the TiO_2 photocatalyst was optimized to improve the yield of the DCC products (Fig. S1). The Pd(5.0)/TiO_2 photocatalyst gave the largest yield of the aromatic DCC products (**1a1** and **1a2**), which is also listed in Table 1, entry 9.

3.2 Mechanistic Studies

3.2.1 Radical Formation

Based on our previous studies on the photocatalytic C–C cross-coupling reactions, [29, 31, 33, 34] the present photocatalytic DCC between toluene and acetone is also considered to involve the hole oxidation of the organic molecules to produce their corresponding radical species and protons. In the present study, the formation of acetonyl radical during the photoirradiation of the Pd/TiO_2 sample was confirmed by the ESR measurements (see Supplementary Information for details). Photoirradiation of a suspension of acetone and a spin trap reagent (DMPO) with the Pd/TiO_2 photocatalyst gave some ESR signals (Fig. 1a). The signals were not obtained without the photocatalyst, acetone, or light irradiation, suggesting that the radical species are produced from acetone upon its oxidation by the photogenerated holes on the TiO_2 photocatalyst.

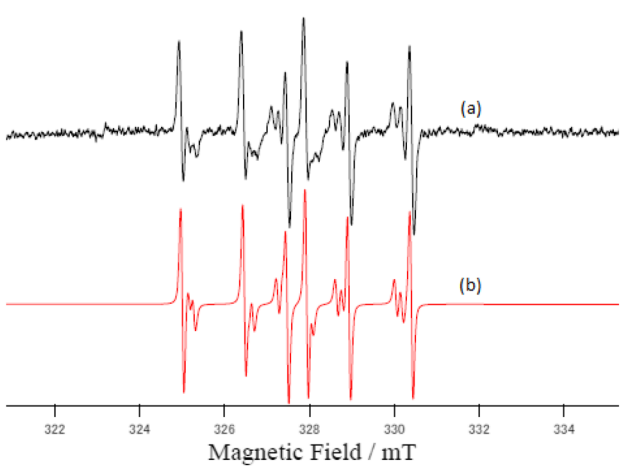

Fig. 1 Experimental (a) and simulated (b) ESR spectra of acetone-DMPO solution with Pd/TiO_2 photocatalyst under the light irradiation. Pd loading amount was 0.75 wt%

The observed spectrum was simulated by using EasySpin [35] (Fig. 1b). Analysis revealed that the observed spectrum couldn't be assigned to a single radical species. It consisted of three sets of a triple-doublet arising from the N and the α-H of DMPO-acetone radical adduct (Eqs. 1 and 2). Further, the spectrum changed with time (data not shown). Based on these results, we conclude that the radical species derived from acetone, trapped by DMPO, might be unstable and thus, have different spatial orientations, which would give individual signals in the ESR spectrum. Due to this complexity, the observed spectrum couldn't be assigned to a particular conformation. However, these results prove that, at least, the acetone molecule is oxidized by the photogenerated holes on the Pd/TiO_2 photocatalyst (Eq. 1).

On the other hand, the observation of 1,2-diphenylethane in the photocatalytic reaction supported the formation of the benzyl radicals from toluene by the oxidation of its methyl group. Thus, the photogenerated holes on TiO_2 could oxidize both toluene and acetone to radical species.

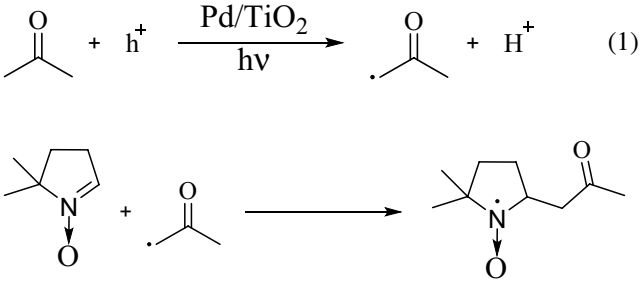

3.2.2 Kinetic Experiments

Next, kinetic experiments were performed to get insight into the reaction mechanism. The photocatalytic reaction tests were done with deuterated acetone (acetone-d_6) and deuterated toluene (toluene-d_8).

Table 2 shows the results of the reaction test carried out with the Pt(0.5)/TiO_2 photocatalyst giving **1b** as the main product. Compared to the reaction done without any deuterated reagent (Table 2, entry 1), the amount of **1b** was significantly decreased in the reaction carried out with deuterated

Table 2 Isotopic experiments for the direct photocatalytic DCC between toluene and acetone with the Pt(0.5)/TiO_2 photocatalyst

Entry	Reactants		**1b** (μmol)	k_H/k_D^a
1	Toluene	Acetone	0.60	–
2	Toluene-d_8	Acetone	0.18	3.3
3	Toluene	Acetone-d_6	0.47	1.3

All reaction conditions were the same as those shown in Table 1

[a] k_H/k_D = [amount of **1b** in the reaction without any isotopic reactant (μmol)]/[amount of **1b** with a isotopic reactant (μmol)]

toluene and the k_H/k_D ratio was clearly larger than unity, indicating a normal kinetic isotope effect (KIE) (Table 2, entry 2). This result suggests that the cleavage of the benzylic C–H bond of toluene to give benzyl radical would be the rate determining step (RDS) for the formation of **1b** in this condition. When the reaction was carried out with deuterated acetone, the reaction rate slightly (20%) reduced and the value of k_H/k_D was a little larger than unity (Table 2, entries 1 and 3). This proposed that the cleavage of the C–H bond of acetone to give acetonyl radical would be the RDS for the **1b** formation in this condition. Thus, it is suggested that both toluene and acetone are activated to form the corresponding radical species and the RDS can be varied when the hydrogen was replaced with deuterium.

Table 3 shows the results obtained with the Pd(5.0)/TiO_2 photocatalyst that gave **1a1** as the major product. The reaction done with deuterated toluene (Table 3, entry 2) gave a small amount of **1a1**, contrary to the reaction done without any isotopic compound (Table 3, entry 1). The value of k_H/k_D was more than unity, corresponding to the normal KIE. The amount of **1a1** remained almost unchanged with the replacement of acetone with deuterated acetone (Table 3, entries 1 and 3). Thus, the value of k_H/k_D was unity. These results and the structure of the 1-(*o*-tolyl)propan-2-one (**1a1**) suggest that the RDS in the production of **1a1** would be the cleavage of the C–H bond of the aromatic ring in toluene. However, the literature has shown that the phenyl radical of toluene is unstable and rapidly converts to benzyl radical [36], i.e., the direct fission of the aromatic C–H bond cannot give **1a1** as a product. Thus, to form **1a1**, toluene should not be oxidized to phenyl radical and rather remain a molecule. This requires that the photocatalytically generated acetonyl radical attacks the toluene molecule. This will lead to a radical transition state which will convert to **1a1** by the elimination of a hydrogen radical, belonging to toluene. So, the aromatic C–H bond of toluene would be broken from the transition state rather than the toluene molecule. As indicated by the isotopic experiments, this elimination of a hydrogen radical from toluene might be the RDS for the formation of **1a1**.

Table 3 Isotopic experiments for the direct photocatalytic DCC between toluene and acetone with the Pd(5.0)/TiO_2 photocatalyst

Entry	Reactants		**1a1** (μmol)	k_H/k_D[a]
1	Toluene	Acetone	2.53	–
2	Toluene-d_8	Acetone	0.98	2.6
3	Toluene	Acetone-d_6	2.57	1.0

All reaction conditions were the same as those shown in Table 1

[a] k_H/k_D = [amount of **1a1** in the reaction without any isotopic reactant (μmol)]/[amount of **1a1** with a isotopic reactant (μmol)]

3.2.3 Temperature-Controlled Photocatalytic Reaction Tests

Several studies have shown that Pd nanoparticles are crucial for the photocatalytic aromatic substitution reactions by carbon centered radicals like acetonitrile [29, 33] and ether. [34, 37] In these reactions, Pd was proposed to have a catalytic role which involves the activation of the aromatic ring to facilitate its reaction with the photogenerated radical species. Besides, Pt nanoparticles are recognized as an efficient electron receiver on TiO_2 photocatalyst to increase the photocatalytic activity. [38, 39] So, to elucidate the different role of Pd and Pt nanoparticles in the formation of **1a1** and **1b**, respectively, we studied the effect of temperature on the photocatalytic DCC between toluene and acetone with the Pd/TiO_2 and Pt/TiO_2 samples at different temperatures. The details are mentioned in the Supplementary Information.

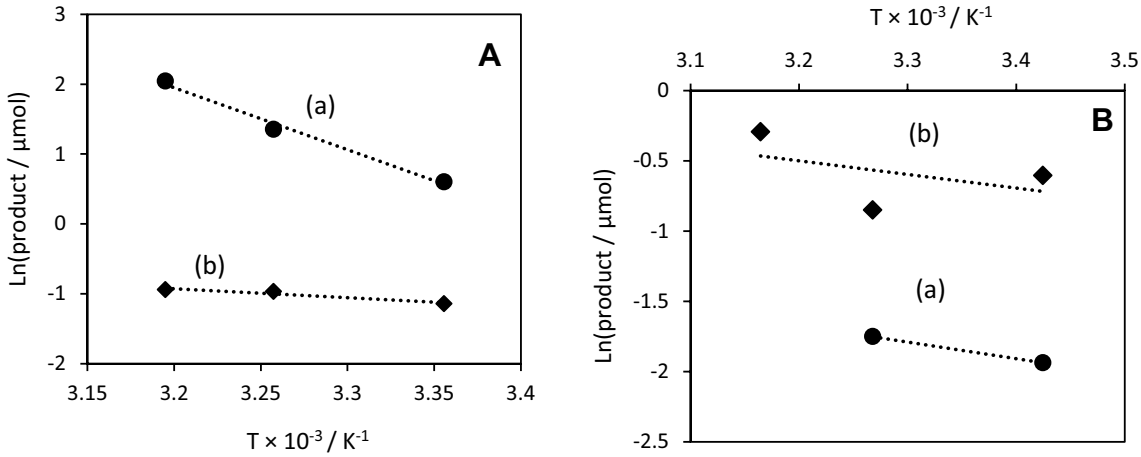

Fig. 2 Pseudo Arrhenius plots of the temperature-controlled photocatalytic DCC between toluene and acetone with the Pd(5.0)/TiO_2 photocatalyst (**A**) and the Pt(0.5)/TiO_2 photocatalyst (**B**), to give **1a1** (a) and **1b** (b)

For the reaction carried out with the Pd(5.0)/TiO_2 sample, the amount of **1a1** steadily increased with temperature while that of **1b** varied only slightly (Fig. 2A, and Table S1, entries 1–3). The apparent activation energies, E_a, calculated from the pseudo Arrhenius plot of this data, were 73 kJ mol^{-1} for **1a1** and 10 kJ mol^{-1} for **1b** (Fig. 2A). No products were formed in the reaction carried out in the dark at high temperature (Table S1, entry 4). Similar experiments were carried out with the Pt(0.5)/TiO_2 sample (Table S1, entries 5–7). The amount of both products did not vary much with temperature and the E_a were 10 and 8 kJ mol^{-1} for both **1a1** and **1b**, respectively (Fig. 2B).

The comparable and small E_a for **1b** with the two samples (Fig. 2A-b and B-b) indicates that, irrespective of the nature of the metal cocatalyst on TiO_2, the formation of **1b** proceeds essentially without thermal energy in a similar way but with photoenergy. Thus, it would be a purely photocatalytic process. The slight increase in the formation rate of **1b** with temperature might be due to some non-catalytic processes like electron migration, electron transfer to metal nanoparticles, and desorption of products from the surface [40].

The E_a for **1a1**, on the other hand, was quite different on the two samples (Fig. 2A-a and B-a). Especially, the value with the Pd/TiO_2 photocatalyst was quite high for a usual photocatalytic process. This suggests the involvement of a certain non-photocatalytic step in this reaction. The formation of **1a1**, as discussed before, is proposed to follow a radical addition–elimination mechanism involving the reaction between acetonyl radical and toluene molecule, catalyzed by the Pd nanoparticles. This step might be further promoted at higher temperature, which will increase the yield of **1a1** (Fig. 2A-a). The small E_a obtained for **1a1** with the Pt/TiO_2 sample indicates, such catalysis is not possible by Pt nanoparticles, which is why the yield of **1a1** is low with the Pt/TiO_2 sample. Thus, the Pd nanoparticles were evidenced to play a catalytic role in the photocatalytic acetonylation of toluene to give **1a1**, where the Pd nanoparticles would absorb and activate the aromatic ring of toluene to react with the acetonyl radical. In contrast, the Pt nanoparticles would function as not a catalyst but an electron receiver to promote the formation of benzyl and acetonyl radicals to give **1b**.

3.2.4 Proposed Reaction Mechanism

Based on these observations, we have proposed the following two mechanisms for the direct photocatalytic DCC between toluene (**1**) and acetone. At first the mechanism for the formation of 1-(*o*-tolyl)propan-2-one (**1a1**) by the Pd/TiO_2 photocatalyst is described (Fig. 3). (i) The photoexcitation of the TiO_2 photocatalyst generates electron and hole. The hole moves to the TiO_2 surface while the

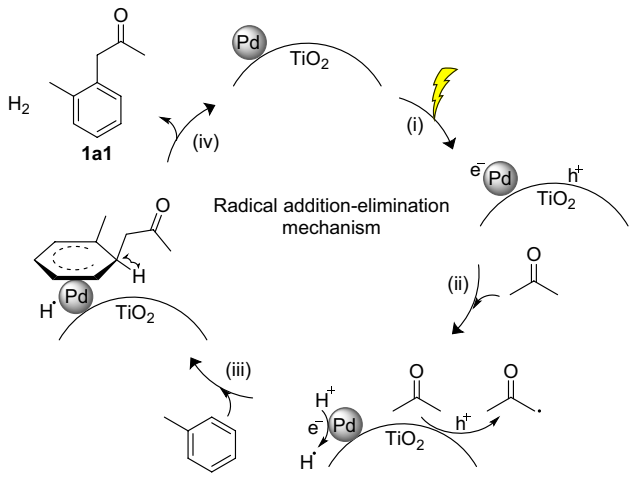

Fig. 3 Proposed reaction mechanism for the direct photocatalytic DCC between toluene and acetone to give **1a1** by the Pd/TiO_2 photocatalyst

electron moves to Pd nanoparticles. (ii) The hole can oxidize an acetone molecule to generate the acetonyl radical species and proton (H^+). The electron on the Pd nanoparticles can reduce the proton to hydrogen radical ($H^{\cdot}$). (iii) The acetonyl radical species can attack the toluene molecule, assisted by the catalysis of Pd nanoparticles, to generate a radical transition state. This is a radical addition–elimination mechanism [29, 33, 34], which is the most important step to change the product selectivity. Here, the acetonyl radical species preferably attacks the *ortho* position. (iv) Elimination of a hydrogen radical from this transition state gives the acetonylated product **1a1**. The two hydrogen radicals can combine to give hydrogen gas. This is a one-photon process. A similar attack of the acetonyl radical at the *para* position in toluene will give **1a2**. Although the mechanism for the **1a1** and **1a2** formation on the Pt/TiO_2 photocatalyst has not clarified because of the low yields, the different activation energy suggested that it takes place via a different mechanism from the Pd/TiO_2 photocatalyst with a slow rate.

Figure 4 shows the mechanism for the formation of 4-phenylbutan-2-one (**1b**) by the Pt/TiO_2 photocatalyst. (i) Photoexcitation of the TiO_2 photocatalyst generates electrons and holes in its conduction and valence band, respectively. The electrons move to the Pt nanoparticles leaving the holes on TiO_2. (ii) The holes can oxidize both methyl group of toluene and acetone to generate their corresponding radical species and protons. The protons can be reduced to hydrogen radicals by the electrons on the Pt surface. (iii) The two organic radical species can combine to give the acetonylated product **1b**, and (iv) the two hydrogen radicals can combine

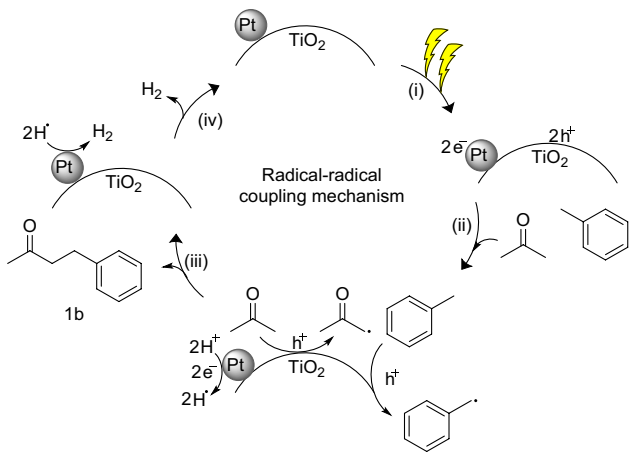

Fig. 4 Proposed reaction mechanism for the direct photocatalytic DCC between toluene and acetone to give **1b** by the Pt/TiO_2 photocatalyst

to release hydrogen gas. This radical–radical coupling mechanism is a two-photon process. The **1b** formation on the Pd/TiO_2 photocatalyst would also follow a similar radical–radical coupling mechanism.

4 Conclusions

In this report, we have accomplished the direct photocatalytic DCC between toluene and acetone to give acetonylated compounds. The nature of the metal cocatalysts deposited on the TiO_2 surface significantly affected the selectivity of the DCC products. Pd promoted the DCC between the aromatic ring of toluene and acetone with high selectivity (94%) via the radical addition–elimination mechanism, which was attributed to the catalytic property of the Pd nanoparticles for the reaction between aromatic ring and organic radical species in the C–C couplings, in other words, the Pd nanoparticles would adsorb and activate the aromatic ring of toluene to react with the acetonyl radical. Pt nanoparticles, on the contrary, promoted the DCC between the methyl group of toluene and acetone with high selectivity (87%) via the radical–radical coupling. The Pt nanoparticles should contribute as an electron receiver to improve the efficiency of this reaction on the TiO_2 photocatalyst.

Although the reported yields are low in the current conditions, this study increased the versatility of TiO_2 photocatalysis in organic synthesis. Further, it highlights the importance and roles of metal cocatalysts in the photocatalytic reaction, that is, their properties can direct the course of the reaction and result in high product selectivity.

Acknowledgements The present project was financially supported by Core Research for Evolutional Science and Technology, Japan Science and Technology Agency (CREST, JST; JPMJCR1541).

References

1. Fujishima A, Honda K (1972) Electrochemical photolysis of water at a semiconductor electrode. Nature 238:37–38. https://doi.org/10.1038/238038a0
2. Abe R, Sayama K, Domen K, Arakawa H (2001) A new type of water splitting system composed of two different TiO_2 photocatalysts (anatase, rutile) and a IO^{3-}/I^{-} shuttle redox mediator. Chem Phys Lett 344:339–344. https://doi.org/10.1016/S0009-2614(01)00790-4
3. Ni M, Leung MKH, Leung DYC, Sumathy K (2007) A review and recent developments in photocatalytic water-splitting using TiO_2 for hydrogen production. Renew Sustain Energy Rev 11:401–425. https://doi.org/10.1016/j.rser.2005.01.009
4. Yanghe F, Dengrong S, Yongjuan C et al (2012) An amine-functionalized titanium metal-organic framework photocatalyst with visible-light-induced activity for CO_2 reduction. Angew Chem Int Ed 51:3364–3367. https://doi.org/10.1002/anie.201108357
5. Mori K, Yamashita H, Anpo M (2012) Photocatalytic reduction of CO_2 with H_2O on various titanium oxide photocatalysts. RSC Adv 2:3165–3172. https://doi.org/10.1039/C2RA01332K
6. Low J, Cheng B, Yu J (2017) Surface modification and enhanced photocatalytic CO_2 reduction performance of TiO_2: a review. Appl Surf Sci 392:658–686. https://doi.org/10.1016/j.apsusc.2016.09.093
7. Fujishima A, Zhang X, Tryk DA (2007) Heterogeneous photocatalysis: from water photolysis to applications in environmental cleanup. Int J Hydrog Energy 32:2664–2672. https://doi.org/10.1016/j.ijhydene.2006.09.009
8. Di Paola A, García-López E, Marcì G, Palmisano L (2012) A survey of photocatalytic materials for environmental remediation. J Hazard Mater 211–212:3–29. https://doi.org/10.1016/j.jhazmat.2011.11.050
9. Fagnoni M, Dondi D, Ravelli D, Albini A (2007) Photocatalysis for the formation of the C–C bond. Chem Rev 107:2725–2756. https://doi.org/10.1021/cr068352x
10. Ma D, Liu A, Li S et al (2018) TiO_2 photocatalysis for C–C bond formation. Catal Sci Technol 8:2030–2045. https://doi.org/10.1039/C7CY01458A
11. Li R, Kobayashi H, Guo J, Fan J (2011) Visible-light induced high-yielding benzyl alcohol-to-benzaldehyde transformation over mesoporous crystalline TiO_2: a self-adjustable photo-oxidation system with controllable hole-generation. J Phys Chem C 115:23408–23416. https://doi.org/10.1021/jp207259u
12. Xianjun L, Hongwei J, Chuncheng C et al (2011) Selective formation of imines by aerobic photocatalytic oxidation of amines on TiO_2. Angew Chem Int Ed 50:3934–3937. https://doi.org/10.1002/anie.201007056
13. Yamamoto A, Ohara T, Yoshida H (2018) Visible-light-induced photocatalytic benzene/cyclohexane cross-coupling utilizing a ligand-to-metal charge transfer benzene complex adsorbed on titanium oxides. Catal Sci Technol 8:2046–2050. https://doi.org/10.1039/c7cy02566a
14. Ikeda S, Ikoma Y, Kobayashi H et al (2007) Encapsulation of titanium(iv) oxide particles in hollow silica for size-selective photocatalytic reactions. Chem Commun 3753–3755. https://doi.org/10.1039/B704468B
15. Yurdakal S, Palmisano G, Loddo V et al (2008) Nanostructured rutile TiO_2 for selective photocatalytic oxidation of aromatic alcohols to aldehydes in water. J Am Chem Soc 130:1568–1569. https://doi.org/10.1021/ja709989e
16. Sofianou M-V, Psycharis V, Boukos N et al (2013) Tuning the photocatalytic selectivity of TiO_2 anatase nanoplates by altering

the exposed crystal facets content. Appl Catal B 142–143:761–768. https://doi.org/10.1016/j.apcatb.2013.06.009
17. Selvam K, Swaminathan M (2011) Cost effective one-pot photocatalytic synthesis of quinaldines from nitroarenes by silver loaded TiO_2. J Mol Catal A 351:52–61. https://doi.org/10.1016/j.molcata.2011.09.014
18. Zheng Z, Huang B, Qin X et al (2011) Facile in situ synthesis of visible-light plasmonic photocatalysts M@TiO_2 (M = Au, Pt, Ag) and evaluation of their photocatalytic oxidation of benzene to phenol. J Mater Chem 21:9079–9087. https://doi.org/10.1039/C1JM10983A
19. Alfè M, Spasiano D, Gargiulo V et al (2014) TiO_2/graphene-like photocatalysts for selective oxidation of 3-pyridine-methanol to vitamin B3 under UV/solar simulated radiation in aqueous solution at room conditions: the effect of morphology on catalyst performances. Appl Catal A 487:91–99. https://doi.org/10.1016/j.apcata.2014.09.002
20. Kou J, Lu C, Wang J et al (2017) Selectivity enhancement in heterogeneous photocatalytic transformations. Chem Rev 117:1445–1514. https://doi.org/10.1021/acs.chemrev.6b00396
21. Tanaka A, Fuku K, Nishi T et al (2013) Functionalization of Au/TiO_2 plasmonic photocatalysts with pd by formation of a core–shell structure for effective dechlorination of chlorobenzene under irradiation of visible light. J Phys Chem C 117:16983–16989. https://doi.org/10.1021/jp403855p
22. Zou X, Tao Z, Asefa T (2013) Semiconductor and plasmonic photocatalysis for selective organic transformations. Curr Org Chem 17:1274–1287. https://doi.org/10.2174/1385272811317120004
23. Wang F, Li C, Chen H et al (2013) Nanogold plasmonic photocatalysis for organic synthesis and clean energy conversion. Chem Soc Rev 43:7188–7216. https://doi.org/10.1021/ja310501y
24. Wu X, Jaatinen E, Sarina S, Zhu HY (2017) Direct photocatalysis of supported metal nanostructures for organic synthesis. J Phys D 50:283001. https://doi.org/10.1088/1361-6463/aa73f6
25. Allen A, Cantrell TS (1989) Synthetic reductions in clandestine amphetamine and methamphetamine laboratories: a review. Forensic Sci Int 42:183–199. https://doi.org/10.1016/0379-0738(89)90086-8
26. Newman MS, Booth WT (1945) The preparation of ketones from grignard reagents. J Am Chem Soc 67:154. https://doi.org/10.1021/ja01217a503
27. Shatzmiller S, Lidor R, Shalon E, Bahar E (1984) A novel route to arylacetones via a masked [small alpha]-acylcarbonium intermediate. J Chem Soc Chem Commun 795–796. https://doi.org/10.1039/C39840000795
28. Yinghuai Z, Bahnmueller S, Hosmane NS, Maguire JA (2003) An effective system to synthesize arylacetones. Substrate-ionic liquid-ultrasonic irradiation. Chem Lett 32:730–731. https://doi.org/10.1246/cl.2003.730
29. Wada E, Takeuchi T, Fujimura Y et al (2017) Direct cyanomethylation of aliphatic and aromatic hydrocarbons with acetonitrile over a metal loaded titanium oxide photocatalyst. Catal Sci Technol 7:2457–2466. https://doi.org/10.1039/c7cy00365j
30. Wada E, Tyagi A, Yamamoto A, Yoshida H (2017) Dehydrogenative lactonization of diols with a platinum-loaded titanium oxide photocatalyst. Photochem Photobiol Sci 16:1744–1748. https://doi.org/10.1039/C7PP00258K
31. Tyagi A, Yamamoto A, Kato T, Yoshida H (2017) Bifunctional property of Pt nanoparticles deposited on TiO_2 for the photocatalytic sp^3 C–sp^3 C cross-coupling reactions between THF and alkanes. Catal Sci Technol 7:2616–2623. https://doi.org/10.1039/C7CY00535K
32. Naniwa S, Tyagi A, Yamamoto A, Yoshida H (2018) Visible-light photoexcitation of pyridine surface complex, leading to selective dehydrogenative cross-coupling with cyclohexane. Phys Chem Chem Phys 20:28375–28381. https://doi.org/10.1039/c8cp04292f
33. Yoshida H, Fujimura Y, Yuzawa H et al (2013) A heterogeneous palladium catalyst hybridised with a titanium dioxide photocatalyst for direct C–C bond formation between an aromatic ring and acetonitrile. Chem Commun 49:3793–3795. https://doi.org/10.1039/c3cc41068d
34. Tyagi A, Matsumoto T, Kato T, Yoshida H (2016) Direct C–H bond activation of ethers and successive C–C bond formation with benzene by a bifunctional palladium–titania photocatalyst. Catal Sci Technol 6:4577–4583. https://doi.org/10.1039/C5CY02290H
35. Stoll S, Schweiger A (2006) EasySpin, a comprehensive software package for spectral simulation and analysis in EPR. J Magn Reson 178:42–55. https://doi.org/10.1016/j.jmr.2005.08.013
36. Childress BC, Rice AC, Shevlin PB (1974) Rearrangement of the o-tolyl radical to the benzyl radical. CIDNP [chemically induced dynamic nuclear polarization] study. J Org Chem 39:3056–3058. https://doi.org/10.1021/jo00934a030
37. Tyagi A, Yamamoto A, Yoshida H (2018) Novel blended catalysts consisting of a TiO_2 photocatalyst and an Al_2O_3 supported Pd–Au bimetallic catalyst for direct dehydrogenative cross-coupling between arenes and tetrahydrofuran. RSC Adv 8:24021–24028. https://doi.org/10.1039/c8ra02948b
38. Ward MD, Bard AJ (1982) Photocurrent enhancement via trapping of photogenerated electrons of titanium dioxide particles. J Phys Chem 86:3599–3605. https://doi.org/10.1021/j100215a021
39. Jovic V, Al-Azri ZHN, Chen W-T et al (2013) Photocatalytic H_2 production from ethanol-water mixtures over Pt/TiO_2 and Au/TiO_2 photocatalysts: a comparative study. Top Catal 56:1139–1151. https://doi.org/10.1007/s11244-013-0080-8
40. Shimura K, Maeda K, Yoshida H (2011) Thermal acceleration of electron migration in gallium oxide photocatalysts. J Phys Chem C 115:9041–9047. https://doi.org/10.1021/jp110824n